Investigation of turbulence properties via spectral broadening of Doppler reflectometry signals in ASDEX Upgrade

G.D.Conway[1], C.Lechte[2], P.Hennequin[3], P.Simon[1,2,4], and the ASDEX Upgrade Team

[1] *Max-Planck Institut für Plasmaphysik, 85748 Garching, Germany*

[2] *IGVP, Universität Stuttgart, 70569 Stuttgart, Germany*

[3] *Laboratoire de Physique des Plasmas, Ecole Polytechnique, 91128 Palaiseau, France*

[4] *Institut Jean Lamour, Université de Lorraine, 54011 Nancy, France*

1. Introduction

Doppler reflectometry (backscatter, BS) is an established microwave diagnostic technique for measuring plasma flows and turbulence in magnetically confined plasmas with sub-millisecond temporal and mm spatial (radial) resolution. Fig. 1 shows a typical signal spectrum from an ASDEX Upgrade (AUG) L-mode edge plasma (limiter, $B_T = -2.2$ T, $\bar{n}_{eo} \approx 2.5 \times 10^{19}$ m^{-3}) using an X-mode, $50 - 75$ GHz stepped frequency reflectometer [1]. From the Doppler shift f_D (obtained by Gaussian fit to the asymmetric spectral component [1]) the turbulence velocity $u_\perp = v_{E\times B} + v_{ph} = 2\pi f_D/k_\perp$ is extracted. $k_\perp = 2N_\perp k_o$ is the turbulence wavenumber at the beam turning point, obtained from beam-tracing (TORBEAM). Further, the peak power A_D, or rather the integrated peak $S(k_\perp) \propto A_D \cdot w_D$, gives a measure of the turbulence level $|\delta n|^2$ at the probed $k_\perp$. Here w_D is the $1/e$ power spectral half-width, usually assumed to be determined by the diagnostic wavenumber resolution $\delta k_\perp$, set by the probing beam width/divergence and curvature effects [2]. However, in AUG, w_D is much wider than expected from the intrinsic $\delta k_\perp$ alone. In fact, peak broadening may arise from several factors: turbulent and coherent flow oscillations, such as GAMs; flow shear; non-linear turb. interactions; as well as beam spreading from low k forward-scattering (FS). These effects are investigated with an eye to the turbulence properties.

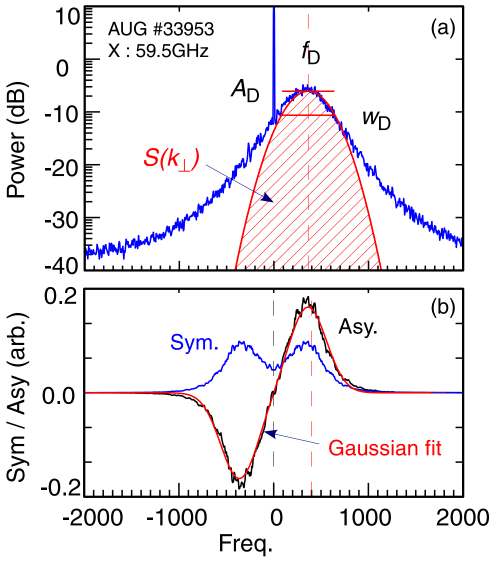

Fig. 1: (a) Typical Doppler refl. spectrum from AUG edge with (b) symmetric and asymmetric components.

2. Doppler $k_\perp$ resolution

Fig. 2(a) shows a radial profile of the intrinsic diagnostic $\delta k_\perp$ for the L-mode shot #33953, obtained with the IPF-FD3D full-wave FDTD code [3]. The O and X-mode 2D simulations use experimental equilibria, antenna geometry and density profiles as input, and produce 2D maps of the wave E^2 field. Taking a Fourier transform of the field pattern along a poloidal slice through the beam turning point gives the (ideal, no turbulence) instrument response - i.e. replicating a real reflectometer measurement [4]. $\delta k_\perp$ is the $1/e$ half-width

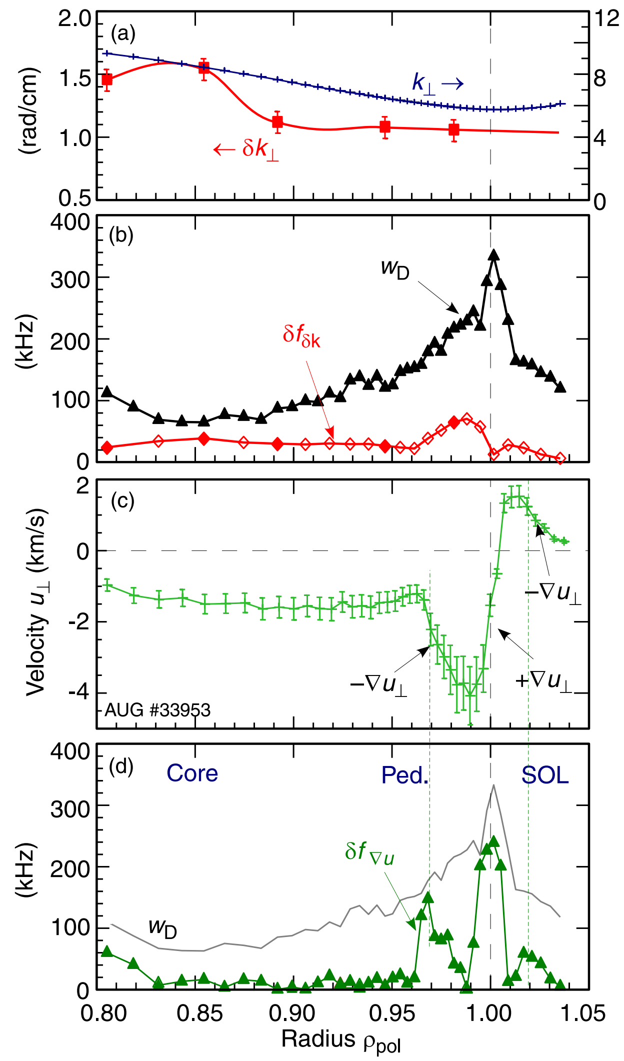

Fig. 2: (a) full-wave $\delta k_\perp$ and ray-trace $k_\perp$, (b) $\delta f_{\delta k}$ (diamonds) & measured w_D (triangles), (c) $u_\perp$ and (d) shear $\delta f_{\nabla u}$: Limiter L-mode #33953.

of the E^2 k-spectral power, which ranges between $0.7 - 1.5$ rad/cm. Converting to $\delta f_{\delta k} = u_\perp \delta k_\perp / 2\pi$ gives the red points in fig. 2(b). Compared with the measured Doppler peak width w_D (black) $\delta f_{\delta k} < w_D$ by a factor of $5 - 10$ or more. This is a general feature of all AUG shots and is particularly evident around the separatrix where the $u_\perp$ velocity reverses, fig. 2(c) and $\delta f_{\delta k}$ dips, but w_D peaks.

3. Flow shear & radial resolution

The peak in w_D at the separatrix may be explained by the finite volume of the Doppler backscatter region around the beam turning point. In regions of strong radial shear in $u_\perp$ this results in a smearing of the Doppler shift [5] (f_D broadening but no peak splitting in AUG L-mode), the magnitude of which may be estimated via $\delta f_{\nabla u} = \nabla u_\perp \Delta r \, k_\perp / 2\pi$ where $\nabla u_\perp$ is the velocity gradient and Δr the diagnostic radial resolution. Here, the radial extent is estimated as the fwhm of the first Airy lobe of E^2, obtained from the 2D full-wave simulations by taking a radial slice through the beam turning point. For a range of AUG simulations the lobe width is found to be in reasonable agreement with the 1D formula $\Delta r = 1.63 \, L_\epsilon^{1/3} \, k_o^{-2/3}$, where $L_\epsilon = (dN^2/dr)^{-1}$ is the dielectric constant scale length at the beam turning point [4,6]. The example in fig. 2(d) shows the strong negative and positive $u_\perp$ shear regions account largely for the magnitude and shape of the w_D peaks. However, the flow shear does not explain w_D in the SOL or in the E_r well.

4. Flow perturbations - coherent & random

In the L-mode edge region (usually between pedestal and separatrix) there is strong GAM activity. The GAM is a few kHz coherent $E \times B$ flow oscillation, shown in the f_D spectra in fig. 3(a), which can reach magnitudes of $10 - 30\%$ of $u_\perp$ on the tokamak outboard plane. The p.t.p. contribution of the GAM $u_\perp$ modulation may be estimated directly by integrating the GAM peak in the f_D fluctuation spectra [7]. The resulting $\delta f_{\rm GAM}$ are shown as crosses in fig. 3(c). Although $\delta f_{\rm GAM} < w_D$ it adds to $\delta f_{\delta k}$ and thus the GAM can make a significant contribution when present. Also shown in fig. 3(c) is the broadband

$\tilde{f}_D$ standard deviation σ_{f_D}, i.e. the total f_D spectral integral, with GAM. σ_{f_D} includes the turbulence mutation (see below) i.e. forward cascade, as well as the non-linear turbulence/zonal-flow interaction. While σ_{f_D} tends to follow w_D in the edge (qualitatively), there is a notable dip in σ_{f_D} when the GAM is present. Away from the GAM region, i.e. around the E_r well, the SOL, and inside of the pedestal top, where the flow shear is weak and the GAM is suppressed, the f_D spectra show a broad enhancement of the random flow perturbations. In the SOL, low frequencies dominate the spectra, which tends to $1/f$-like, while the core flow spectra are more flat.

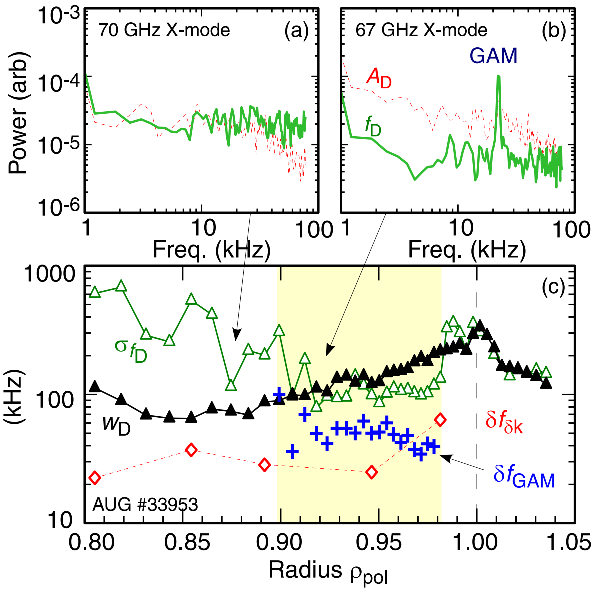

Fig. 3: (a,b) Flow $\tilde{f}_D$ and turb. $\tilde{A}_D$ spectra, (c) w_D (black), $\delta f_{\rm GAM}$ (crosses), σ_{f_D} (green) for limiter L-mode #33953.

5. Zero-frequency peaks & Forward-scattering

Towards the core both the w_D and the random flow σ_{f_D} increase again (as seen in fig. 3(c), and more clearly in fig. 4 for the high density $\bar{n}_{eo} = 7 \times 10^{19}$ m^{-3}, 1 MA, $B_T = -2.5$ T, lower-single-null, NBI heated L-mode, with O and X-mode probing) although the turbulence falls progressively, as shown by the Doppler peak intensity $A_D.w_D$ (filled) and the σ_{A_D} (open symbols). The peak broadening in the core is often accompanied by the appearance of a 2nd spectral peak close to zero frequency with a fairly constant amplitude and width w_o (fig. 4(a) blue points) in radius. The zero-frequency peak generally only becomes evident when the main Doppler BS peak is both weak (i.e. low turbulence, $\sim 15-20$ dB down on edge values - cf. fig. 4) and well shifted in frequency, as shown in the example spectrum of fig. 5(a) with peaks of comparable magnitude. A zero-frequency peak can arise from a direct beam reflection from in-vessel components (not evident here), or an antenna side-lobe radiating at normal incidence to the plasma. However, as shown by the beam-tracing plot in fig. 5(b) for the 71 GHz O-mode case of fig. 4, the main beam incidence angle is rather large, requiring $k_\perp \sim 0$ side-lobe reflections at $\sim 15-17°$ to be more than 30 dB stronger than the $k_\perp \approx 10$ cm^{-1} Doppler BS.

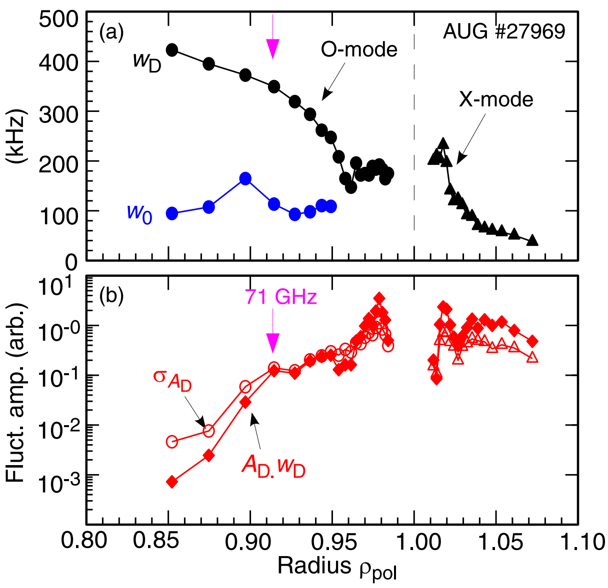

Fig. 4: (a) w_D (black) and w_o (blue) and (b) Doppler peak $A_D \cdot w_D \propto |\delta n|^2$ and fluctuation σ_{A_D} profiles for LSN L-mode #27969.

An additional effect is *non-localized*, small-angle FS and large angle BS of the beam due to low-k turbulence along the beam path [8,9]. The BS may create a zero/low-frequency peak while the FS can lead to beam broadening [10], thus modifying the intrinsic δk, or in extreme cases to complete distortion of the beam phase-front etc. A low-k BS induced peak would suggest FS broadening may also be present. Note, around the beam turning point there is also a *localized* non-zero k_r sensitivity due to the finite scattering volume.

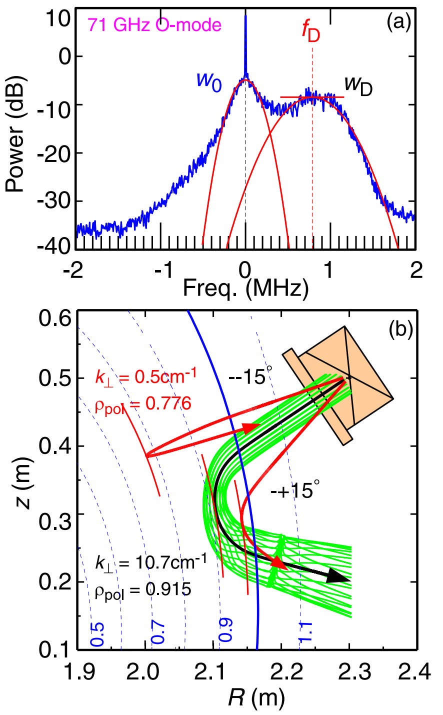

Fig. 5: (a) Doppler spectra and (b) beam-trace plus side-lobe rays, for 71 GHz (O), LSN L-mode #27969.

6. Non-linear interactions

Linear, single-scattering should prevail in the weakly turbulent core region. But, as the beam traverses the more turbulent edge, nonlinear, small-angle multiple-scattering can impact the beam, enhancing the above effects [8,9]. However, numerical estimates indicate the non-linear threshold is not exceeded for the cases here. Finally, the turbulence itself has an intrinsic mutation rate or correlation time, which translates directly to a broadening of the Doppler frequency peak [11]. It may appear as a random (diffusive-like) $\tilde{f}_D$ with a more Lorentzian, rather than pure Gaussian line profile. Its effect will be more evident when $u_\perp$ is small (low convection rate), as in the L-mode cases studied here. The turbulence mutation essentially accounts for the missing component in the measured w_D.

7. Conclusion

Various effects impact the Doppler peak w_D in different regions. After accounting for these effects (if possible), the excess w_D may give information on the intrinsic turbulence diffusive profile, which is important in the study of turbulent transport [11]. A direct comparison of experimental data with non-linear modelling [9] is currently in progress.

References

[1] G.D.Conway *et al.* Plasma Fusion Res. **5**, S2005 (2010)
[2] M.Hirsch & E.Holzhauer, Plasma Phys. Control. Fusion **46**, 593 (2004)
[3] C.Lechte *et al.* Plasma Phys. Control. Fusion **59**, 075006 (2017)
[4] G.D.Conway *et al.* Proc. 12th Intl. Reflectometer Workshop (Jülich) IRW12 (2015)
[5] F.da Silva *et al.* Nucl. Fusion **46**, S816 (2006)
[6] I.H.Hutchinson, Plasma Phys. Control. Fusion **34**, 1225 (1992)
[7] G.D.Conway *et al.* Plasma Phys. Control. Fusion **50**, 085005 (2008)
[8] E.Z.Gusakov & A.V.Surkov, Plasma Phys. Control. Fusion **46**, 1143 (2004)
[9] A.V.Surkov, Plasma Phys. Control. Fusion **48**, 901 (2006)
[10] F.da Silva *et al.* IEEE Trans. Plasma Sci. **38**, 2144 (2010)
[11] P.Hennequin *et al.* Proc. 26th EPS Conf. (Maastricht), ECA vol. **23J**, 977 (1999)